BRAIN
A JOURNAL OF NEUROLOGY

REPORT

SLC12A2 variants cause a neurodevelopmental disorder or cochleovestibular defect

Alisdair McNeill,[1,2,3] Emanuela Iovino,[4] Luke Mansard,[5] Christel Vache,[5] David Baux,[5] Emma Bedoukian,[6] Helen Cox,[7] John Dean,[8] David Goudie,[9] Ajith Kumar,[10] Ruth Newbury-Ecob,[11] Chiara Fallerini,[12,13] Alessandra Renieri,[12,13] Diego Lopergolo,[12,13] ⓘFrancesca Mari,[12,13] Catherine Blanchet,[14] Marjolaine Willems,[15] Anne-Francoise Roux,[5] Tommaso Pippucci[16] and Eric Delpire[17]

The *SLC12* gene family consists of *SLC12A1–SLC12A9*, encoding electroneutral cation-coupled chloride co-transporters. *SCL12A2* has been shown to play a role in corticogenesis and therefore represents a strong candidate neurodevelopmental disorder gene. Through trio exome sequencing we identified *de novo* mutations in *SLC12A2* in six children with neurodevelopmental disorders. All had developmental delay or intellectual disability ranging from mild to severe. Two had sensorineural deafness. We also identified *SLC12A2* variants in three individuals with non-syndromic bilateral sensorineural hearing loss and vestibular areflexia. The *SLC12A2 de novo* mutation rate was demonstrated to be significantly elevated in the deciphering developmental disorders cohort. All tested variants were shown to reduce co-transporter function in *Xenopus laevis* oocytes. Analysis of *SLC12A2* expression in foetal brain at 16–18 weeks post-conception revealed high expression in radial glial cells, compatible with a role in neurogenesis. Gene co-expression analysis in cells robustly expressing *SLC12A2* at 16–18 weeks post-conception identified a transcriptomic programme associated with active neurogenesis. We identify *SLC12A2 de novo* mutations as the cause of a novel neurodevelopmental disorder and bilateral non-syndromic sensorineural hearing loss and provide further data supporting a role for this gene in human neurodevelopment.

1 Department of Neuroscience, University of Sheffield, Sheffield, UK
2 Neuroscience Institute, University of Sheffield, Western Bank, Sheffield, UK
3 Sheffield Clinical Genetics Service, Sheffield Children's Hospital NHS Foundation Trust, Sheffield, UK
4 Department of Medical and Surgical Sciences, University of Bologna, Bologna, Italy
5 Laboratory of Molecular Genetics, CHU Montpellier, University of Montpellier, Montpellier, France
6 Roberts Individualized Medical Genetics Center, Children's Hospital of Philadelphia, Philadelphia, USA
7 Regional Clinical Genetics Unit, Birmingham Women's and Children's Hospital NHS Foundation Trust, Mindelsohn Way, Birmingham, UK
8 North of Scotland Genetics Service, Aberdeen Royal Infirmary, Foresterhill, Aberdeen, UK
9 East of Scotland Regional Genetics Service, Level 6, Ninewells Hospital, Dundee, UK
10 Clinical Genetics Unit, Great Ormond Street Hospital, Great Ormond Street, London, UK
11 Bristol Regional Genetics Service, St Michael's Hospital, Southwell Street, Bristol, UK
12 Medical Genetics, University of Siena, Siena, Italy
13 Genetica Medica, Azienda Ospedaliera Universitaria Senese, Siena, Italy
14 Centre of Reference for Genetic Sensory diseases, CHU Montpellier, University of Montpellier, Montpellier, France
15 Department of Clinical Genetics, CHU Montpellier, University of Montpellier, Montpellier, France
16 Medical Genetics Unit, Polyclinic Sant'Orsola-Malpighi University Hospital, Bologna, Italy
17 Department of Anesthesiology, Vanderbilt University School of Medicine, Nashville, TN, USA

[2]Correspondence to: Alisdair McNeill, PhD FRCP Edin DCH
Department of Neuroscience, University of Sheffield, 385a Glossop Road, Sheffield, S10 2HQ, UK
E-mail: a.mcneill@sheffield.ac.uk

[2]Correspondence may also be addressed to: Eric Delpire, PhD
Department of Anesthesiology, Vanderbilt University Medical Center, T-4202 MCN, 1161
21st Avenue South, Nashville, TN 37232-2520, USA
E-mail: eric.delpire@vanderbilt.edu

Introduction

Neurodevelopmental disorders (NDD) affect 1–5% of the population and demonstrate clinical and aetiological heterogeneity (Wright *et al.*, 2015). *De novo* mutations (DNM) are associated with NDD in ∼25% of cases (McRae *et al.*, 2017). Corticogenesis is the process by which neuronal progenitors proliferate and migrate to form the cerebral cortex (Urbán and Guillemot, 2014). Corticogenesis is tightly regulated by transcriptional programmes, with temporal and spatial regulation of gene expression. In humans, corticogenesis begins around embryonic Day 42 and is largely completed by birth (Urbán and Guillemot, 2014). Many of the genes affected by DNM in NDD play a role in corticogenesis (McRae *et al.*, 2017; Zawerton *et al.*, 2019), and corticogenesis genes are strong candidates for NDD. The *SLC12* gene family consists of *SLC12A1–SLC12A9*, encoding electroneutral cation-coupled chloride transporters (Arroyo *et al.*, 2013). Several of these genes are known to cause human disease (Supplementary Table 1). There is no clear gene–disease relationship for *SLC12A2* (NKCC1). However, *SCL12A2* has been shown to play a role in corticogenesis (Young *et al.*, 2012) and the excitatory-inhibitory GABA switch during brain development (He *et al.*, 2014). *SLC12A2* represents a good candidate gene for NDD.

Study of an *Slc12a2*/NKCC1 null mouse demonstrated that the transporter is a key mechanism in the accumulation of the K$^+$-rich endolymph in the inner ear (Delpire *et al.*, 1999). Absence of NKCC1 causes sensorineural deafness and balance deficits. Little is known about a brain phenotype in the NKCC1 knockout mouse. However, NKCC1 expression in central neurons is developmentally regulated in rodents (Plotkin *et al.*, 1997). Expression is likely highest when the neurons are born in the subventricular zone at a time when the intracellular chloride (Cl$^-$) concentration is highest (Ben-Ari, 2012). High Cl$^-$ facilitates the development of GABA-mediated giant synaptic potentials, by which GABA excites developing neurons to promote growth and synapse formation when glutamatergic inputs have not yet developed (Ben-Ari, 2012). Disruption of NKCC1 expression during development is likely to have consequences for brain development.

SLC12A2 undergoes alternative splicing, with eight isoforms identified by the Genotype-Tissue Expression Project (GTEx) (Supplementary Fig. 1) (Stranger *et al.*, 2017). The full-length isoform is 27 exons, with exon 21 being spliced out in the other major isoform. In mouse cochlea, only the exon 21-containing isoform is expressed (Dixon *et al.*, 1999). Deafness in the *sy* mouse is due to an exon 21 frameshift in *Slc12a2* (Dixon *et al.*, 1999). In the brain, both exon 21-containing and exon 21-deleted isoforms are expressed (Morita *et al.*, 2014). Here, we describe six patients with DNM in *SLC12A2* associated with an NDD and three with bilateral sensorineural hearing loss (BLSNHL) and exon 21 variants.

Materials and methods

Ascertainment of individuals with *SCL12A2* variants

Probands with protein altering single nucleotide variants (SNVs) in *SLC12A2* were identified in Patients 1–5 by exome sequencing in the Deciphering Developmental Disorders study (DDD) (Wright *et al.*, 2015). Subjects 6–9 were identified via Genematcher (Sobreira *et al.*, 2015). Written consent was obtained from parents/guardians.

In silico assessment of pathogenicity of *SCL12A2* variants

The effects of *SLC12A2* variants were assessed using multiple *in silico* tools (Schwarz *et al.*, 2010; Shihab *et al.*, 2013). The excess in occurrence of *de novo SLC12A2* protein-altering variants in DDD was assessed using DenovolyzeR (Ware *et al.*, 2015), which compares the observed: expected number DNMs to identify an elevated *de novo* mutation rate for a given gene. Spatial clustering of missense *SLC12A2* DNMs was assessed using Denovonear, which calculates the probability of the observed spatial pattern of DNM arising by chance. We used MuPIT, which maps the effect of SNVs onto 3D-protein structures, to visualize the structural effects of DNMs (Niknafs *et al.*, 2013).

Transcriptomic study of *SLC12A2* expression in the developing human brain

Variations in *SLC12A2* transcript levels in the human brain among different developmental stages and anatomical

regions were investigated using data from the BrainSpan Atlas of the Developing Human Brain (Miller *et al.*, 2014). Single cell RNA (scRNA) sequencing data from the human brain at 16–18 weeks gestation were obtained from Pollen *et al.* (2015). NetworkAnalyst, which uses protein-protein interaction networks to analyse gene expression studies, was used to explore transcriptomic differences in scRNA data between *SLC12A2* expressing and non-expressing cells (Xia *et al.*, 2015).

In silico study of expression of *SLC12A2* splice isoforms

RNA-seq data from the BrainSpan Atlas of the Developing Human Brain were used to analyse levels of *SLC12A2* exon expression during brain development. RNA-seq data from developing mouse cochlea were examined for alternative splicing of *SLC12A2* during cochlear development (Ranum *et al.*, 2019).

In vitro assessment of NKCC1 ion transporter function

NKCC1 function was assessed through K^+ influx measurements into *Xenopus laevis* oocytes injected with wild-type or mutant NKCC1 cRNA. Detailed protocols have been published and summarized in the Supplementary material (Delpire *et al.*, 2011).

Data availability

Exome sequencing data from the DDD study are available at the European Genome-Phenome Archive (https://ega-archive.org/studies/EGAS00001000775).

Results

Identification of *SLC12A2* variants in children with neurodevelopmental disorders

Through trio exome sequencing, we identified six children with NDD and DNM in *SLC12A2*. Detailed clinical reports are provided in the Supplementary material and Table 1. All had intellectual disability or developmental delay varying from mild to severe. Three had an autistic spectrum disorder. Patient 1 had cerebral cortical dysplasia on brain MRI. Patient 5 had agenesis of the corpus callosum. Two had BLSNHL. Patient 4 had spastic diplegia and Patient 5 had spastic quadriparesis. In addition we identified three individuals from two unrelated families with congenital nonsyndromic BLSNHL and an *SCL12A2* variant (Table 1). There was no shared facial dysmorphology. None had a pathogenic copy number variant, any additional candidate DNM (Supplementary Table 2) or causal variant in a deafness gene.

In silico assessment of *SLC12A2* variants supports pathogenicity

Seven of the eight identified *SLC12A2* variants were *de novo* and all had Combined Annotation Dependent Depletion (CADD) scores >20 (Table 1 and Fig. 1A). The missense variants affected evolutionarily conserved residues, conserved between *SLC12* gene family members (Supplementary Fig. 2). We assessed whether the DNM rate in the DDD cohort was elevated. We collected all eight *SLC12A2* protein-altering DNMs (the five pathogenic variants plus three variants predicted to be benign) in DDD (Supplementary material). Using DenovolyzeR, we showed a 9.62-fold DNM enrichment in *SLC12A2* ($P = 2.71 \times 10^{-6}$, after correction for multiple testing $P = 0.05$).
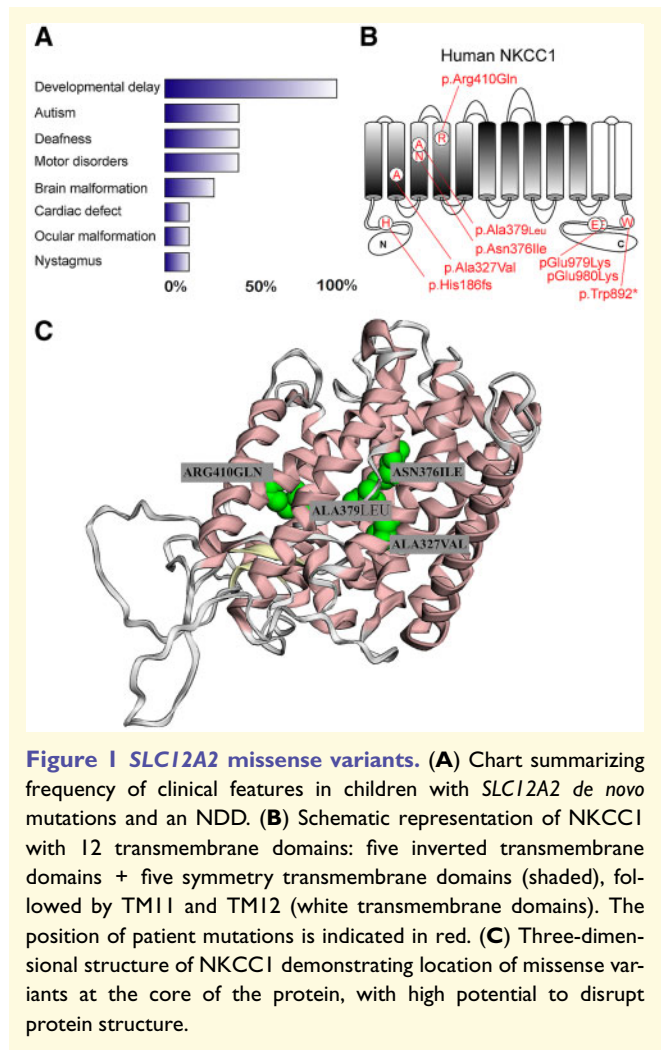
SLC12A2 sequence data from the gnomAD database demonstrated significant constraint for protein-truncating variants in *SLC12A2* [58.7 expected versus 11 observed, pLI = 0.96, observed: expected 0.19 (0.12–0.31)], but not for missense SNVs [594 observed versus 430 expected, Z = 2.4, observed: expected 0.72 (0.67–0.78)]. We then used gnomAD data to examine the spatial distribution of missense SNVs in *SLC12A2*, to look for differential prevalence of missense variants in protein domains (implying regional constraint). There was no difference in the percentage of residues with a synonymous variant in the functionally important domains (transmembrane domains) (Chen *et al.*, 2019) and domains of no known function (19% versus 22%, $P = 0.13$). In the functionally significant domains, 35% of residues had a missense variant compared to 43% of residues in the domains of no known functional significance (chi-squared, $P = 0.0037$). In addition, constraint data from Samocha *et al.* (2017) indicate that amino acids 1–836 are depleted of missense variants (observed 173, expected 294.8, ratio 0.58, chi-squared 50.3) while the remainder of the protein is not. This suggests constraint of missense variation in the functionally significant domains of *SLC12A2*.

Pathogenic *SLC12A2* variants alter NKCC1 activity

To assess the functional significance of the mutations, we injected wild-type NKCC1 and mutant NKCC1 cRNAs in *Xenopus laevis* oocytes and performed standard K^+ influx measurements under isotonic (basal) and hypertonic (stimulated) conditions. We used the mouse cDNA, which is 95% conserved compared to human *SLC12A2*. For every mutation tested, Supplementary Fig. 2 demonstrates homology of the mutated and surrounding residues within the *Slc12a* transporter family and among NKCC1 proteins from six species (sea urchin and five vertebrates). All tested mutations demonstrated significant reduction in K^+ influx (Fig. 2 and detailed results in the Supplementary material).

Table 1 Summary of clinical and genomic data for SLC12A2 variant carriers

	Case 1	Case 2	Case 3	Case 4	Case 5	Case 6	Case 7	Case 8	Case 9
Age, years; sex	1; Male	9; Male	15; Female	3; F	6; F	21; Male	2; Male	44; Male	5; Male
Variant (Genome build GRCh-37/hg19)	g.5127450305C>T	g.5127469897G>A	g.5127503511G>A	g.5127466837A>T	g.5127420201dup	g.5127466845delinsCT	g.5127512805G>A	g.5127512802G>A	g.5127512802G>A
c.DNA variant NM_001046.3	c.980C>T	c.1229G>A	c.2675G>A	c.1127A>T	c.555dupG	c.1135_1136delGCinsCT	c.2938G>A	c.2935G>A	c.2935G>A
ACMG criteria	4	4	5	4	4	4	4	4	4
Inheritance	De novo	De novo	De novo	De novo	De novo	De novo	De novo	Unknown	Inherited from Case 8
Amino acid change	p.(Ala327Val)	p.(Arg410Gln)	p.(Trp892*)	p.(Asn376Ile)	p.(His186AlafsTer17)	p.(Ala379Leu)	p.(Glu980Lys)	p.(Glu979Lys)	p.(Glu979Lys)
Exon (of 27)	4	6	18	5	1	5	21	21	21
gnomAD frequency	0	0.0000070 (2 cases)	0	0	0	0	0	0	0
CADD-Phred score	26.0	31	40	27.3	33	28	23	23	23
GERP	5.36	4.94	4.8	4.92	3.97	4.92	5.11	5.11	5.11
MutationTaster	Disease causing (1)	Disease causing (1)	Disease causing (1)	Disease causing (1)	N/A	Disease causing (1)	Disease causing (1)	Disease causing (1)	Disease causing (1)
FATHMM	Damaging (−5.14)	Damaging (−2.17)	Damaging (0.977) (FATHMM-MKL)	Damaging (−5.18)	N/A	Damaging (−5.03)	Damaging (−1.91)	Damaging (−1.9)	Damaging (−1.9)
PolyPhen-2	Probably damaging (1)	Probably damaging (1)	N/A	Probably damaging (1)	N/A	Probably damaging (1)	Possibly damaging (0.682)	Possibly damaging (0.799)	Possibly damaging (0.799)

Figure 1 SLC12A2 missense variants. (**A**) Chart summarizing frequency of clinical features in children with SLC12A2 de novo mutations and an NDD. (**B**) Schematic representation of NKCC1 with 12 transmembrane domains: five inverted transmembrane domains + five symmetry transmembrane domains (shaded), followed by TM11 and TM12 (white transmembrane domains). The position of patient mutations is indicated in red. (**C**) Three-dimensional structure of NKCC1 demonstrating location of missense variants at the core of the protein, with high potential to disrupt protein structure.

Spatial proximity of SLC12A2 missense de novo mutations altering NKCC1 activity

We wondered whether DNMs [p.(Ala327Val), p.(Arg410Gln), p.(Asn376Ile), p.(Ala379Pro), p.(Glu980Lys)] clustered within the protein. Clustering analysis with Denovonear demonstrated a greater spatial proximity within the protein than expected by chance ($P = 0.027$), with the majority of DNMs falling into transmembrane domains (Fig. 1B). We then used MuPIT to map these DNMs onto NKCC1 3D protein structure, showing all DNMs embedded within the transmembrane core of the protein (Fig. 1C).

Expression of SLC12A2 in developing human brain supports a role in neurogenesis

We next examined SLC12A2 expression in developing human brain using microarray data from the BrainSpan atlas. SLC12A2 expression was significantly higher (Mann-
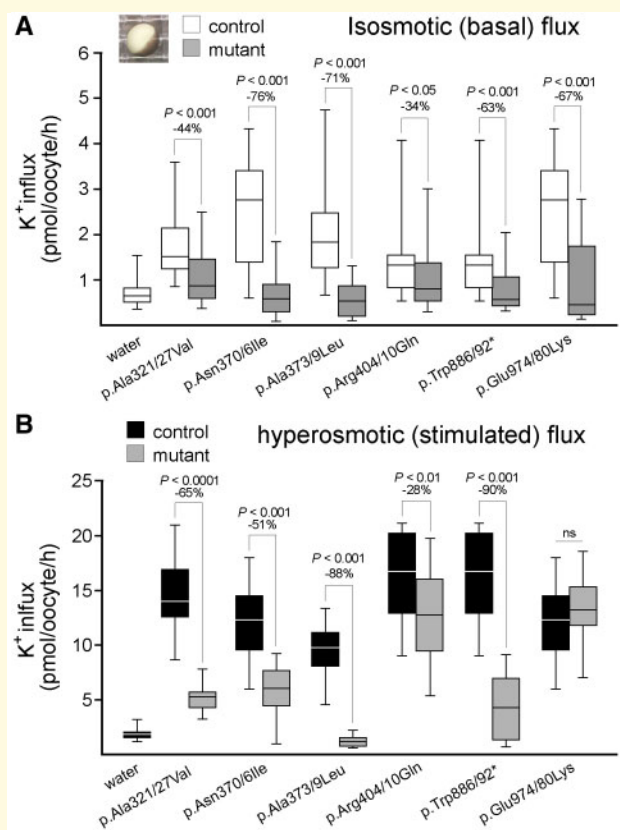
Figure 2 Functional analysis of NKCC1 mutation in *Xenopus laevis* oocytes. (**A** and **B**) Box plots demonstrating K$^+$ influx measured in oocytes injected with water (negative control), water containing 15 ng wild-type (control) or mutant mouse *Slc12a2*/NKCC1 cRNA. Horizontal line represents median, extent of box demonstrates interquartile range and whiskers minimum and maximum. K$^+$ fluxes were measured under basal isosmotic (200 mOsM) or stimulated hyperosmotic (270 mOsM) conditions and are expressed in picomoles K$^+$/oocyte/hour. As the mutants were tested in different experiments on different oocytes, each mutant flux is accompanied by its own control flux. Statistical differences were determined using one-way ANOVA. Each experiment represents 20–25 oocytes per mutation. Note that the mouse residue numbers are slightly different from human.

Figure 3 Transcriptomic analysis of *SCL12A2* expression in developing human brain. (**A**) Box plots of microarray data comparing SLC12A2 expression in neuroanatomical regions of high and less active neurogenesis at 15 weeks gestation. Horizontal lines represent median, extent of box interquartile range and whiskers minimum and maximum. Expression is significantly higher in areas of active neurogenesis (asterisk). (**B**) Single cell RNA sequencing data demonstrating significantly higher expression of *SLC12A2* in radial glia cells (RGC) compared to intermediate progenitor cells (IPC) (Mann-Whitney U-test, Z = –3.3, P = 0.001) and neurons (z = –5.2, P < 0.001). Units are counts per million reads (CPM).

Whitney U-test, Z = –8.36 $P < 0.001$) in neuroanatomical regions with high neurogenesis (ventricular zone, subventricular zone) compared with regions of less active neurogenesis (cortical plate, subplate) at 15–16 weeks gestation (Fig. 3A). For a range of brain expressed genes with no known role in neurogenesis there was no differential expression in neurogenic niches (data not shown).

Single-cell RNA sequencing data from 16–18 weeks gestation foetal brain were then used to identify populations of cells that express *SLC12A2* during development. The marker genes defined by Pollen *et al.* (2015) were used to identify radial glia (e.g. *PAX6*, *SOX2*, *VIM*), intermediate progenitors (e.g. *EOMES*, *RBFOX1*) and neurons (e.g. *MYT1L*, *NEUROD1*, *SATB2*). SLC12A2 expression was
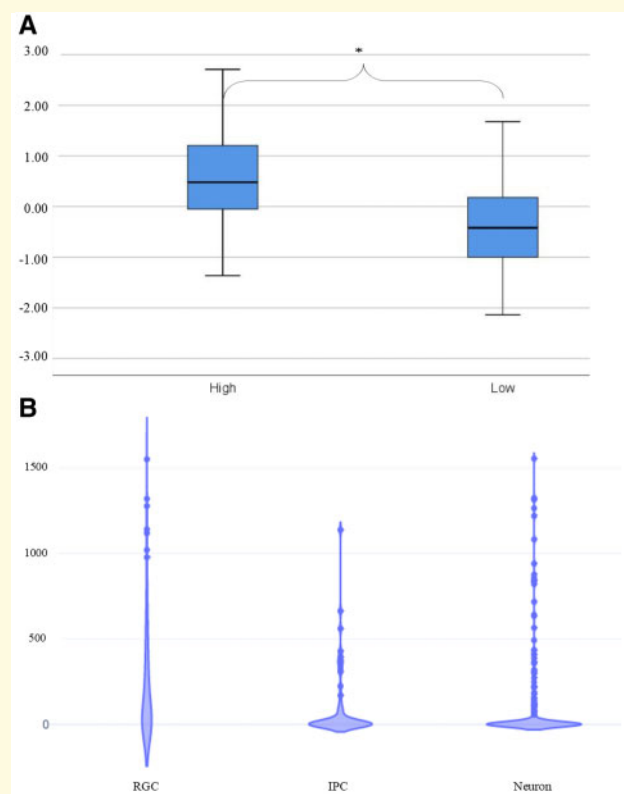
significantly higher in radial glia than in intermediate progenitors (Mann-Whitney U-test, Z = –3.3, P = 0.001) or neurons (z = –5.2, P < 0.001), but did not differ between intermediate progenitors and neurons (z = –1.06, P = 0.28, Fig. 3B). In radial glial there was no expression of other *SLC12* gene family members known to have a role in neuronal development or function. This suggests other *SLC12A2* family members cannot compensate for reduction in *SLC12A2* function associated with *SLC12A2* DNM.

In silico study of expression of *SLC12A2* splice isoforms

RNA-seq data from BrainSpan quantifies levels of exon expression. Supplementary Fig. 3A demonstrates an excess of transcripts for exon 1–28 compared to exon 21 in human

foetal brain. *SLC12A2* isoforms lacking exon 21 therefore exist in developing human brain. RNA-seq of developing mouse cochlea demonstrated no alternative splicing of exon 21; the exon 21-containing isoform is the only transcript expressed (Supplementary Fig. 3B).

SLC12A2 expressing cells display transcriptomic profiles of active neurogenesis

To investigate the functional properties of *SLC12A2* expressing cells we used the single cell RNA sequencing data from Pollen *et al.* (2015) to select cells robustly expressing *SLC12A2* (>100 counts per million) and those with no *SLC12A2* expression. This was done agnostic to cell type. We then used NetworkAnalyst to identify differentially expressed genes in *SLC12A2* expressing cells. This identified 589 differentially expressed genes (corrected *P*-value < 0.05 with > 2-fold difference in expression). Images of networks generated and a full list of enrichment terms is provided in Supplementary Fig. 4.

Given that we were analysing scRNA data from foetal brain, we used tissue-specific (brain cortex) co-expression network analysis to form a network from differentially expressed genes. NetworkAnalyst created a gene co-expression network (Supplementary material). This network was enriched for Reactome terms [e.g. L1CAM interaction and axon guidance (both FDR corrected *P* = 0.00085)] and Gene Ontology (GO) biological process terms [e.g. axonogenesis (*P* = 0.0027), neurodevelopment (*P* = 0.0036)] relevant to neurodevelopment. We then used the label propagation algorithm to identify five modules within the network (Supplementary material). Details of the enrichment analysis of all five modules are provided in the Supplementary material. Module 1 (coloured blue) was the largest (435 genes, Supplementary Fig. 4A). It was enriched for Reactome term 'L1CAM interaction' (*P* = 0.010) and GO biological process terms 'cytoskeleton dependent intracellular transport' (*P* = 0.00005) and 'synaptic transmission' (*P* = 0.00072) as well as Panther biological process term 'nervous system development' (*P* = 0.017). Module 2 (coloured red, 104 genes, Fig. 4B) was enriched for the Reactome term 'notch-HLH transcription pathway' (*P* = 0.0016) and GO biological process terms for 'neuron formation' (neuron differentiation, generation of neurons, neurogenesis, nervous system development, all *P* = 0.01). Modules 3 (coloured white, 123 genes), 4 (coloured green, 117 genes) and 5 (coloured yellow, 123 genes) were not enriched for neurogenesis terms. *SCL12A2* expressing cells manifest a transcriptomic programme suggesting an active role in neurogenesis.

Discussion

We describe six individuals with a pleiotropic NDD associated with DNM in *SCL12A2*. All had developmental delay, ranging from mild to severe. Three had autistic spectrum disorder. In addition, we identified three patients with BLSNHL and no NDD. Two individuals with likely pathogenic variants in *SLC12A2* have previously been reported. We described a female patient with a protein-truncating variant in exon 22 of *SLC12A2* (Delpire *et al.*, 2016). She presented with lung, gastrointestinal tract, endocrine and exocrine gland deficits with seizure-like episodes and EEG abnormalities, but no hearing impairment. Recently, a 5-year-old male with uniparental disomy for chromosome 5 with a 22 kb deletion of *SLC12A2* was described with bilateral sensorineural deafness, global developmental delay and failure to thrive (Macnamara *et al.*, 2019). Our report confirms that *SLC12A2* variants are associated with a pleiotropic NDD and exon 21 variants with BLSNHL.

Pleiotropy is well recognized in NDD (McRae *et al.*, 2017). The explanation for pleiotropy associated with *SLC12A2* is unclear. The severe phenotype in the boy reported by MacNamara *et al.* (2019) is likely related to the presence of a homozygous variant in *SLC12A2*, combined with the effects of uniparental disomy for chromosome 5. Patients 3 and 5 in our series had protein truncating variants and their phenotypes were subjectively more severe than those of the patients with missense variants. A larger series of *SLC12A2* variants will be required to confirm any genotype-phenotype correlation. Patient 7 was 47, XYY. The contribution of this is not clear. XYY syndrome has been associated with a mild reduction in IQ (Green *et al.*, 2019). There is no clear association between BLSNHL or tongue fasciculations and XYY syndrome. The cochlea expresses only the *SLC12A2* isoform containing exon 21, suggesting exon 21 plays a critical developmental role in cochlea (Dixon *et al.*, 1999) and explaining why exon 21 variants cause BLSNHL. Notably, deafness in the *sy* mouse is due to an exon 21 *Slc12a2* mutation (Dixon *et al.*, 1999). In human foetal brain, significant amounts of the *SLC12A2* isoform lacking exon 21 are expressed (Morita *et al.*, 2014). This may compensate for deleterious effects of exon 21 variants and explain why exon 21 variants do not cause an NDD.

In both murine models (Magalhães and Rivera, 2016) and cell systems (Young *et al.*, 2012), loss of *Slc12a2*/NKCC1 has been shown to inhibit neurogenesis. *SLC12A2* is highly expressed in areas of active neurogenesis and *SLC12A2* expression is higher in radial glia than in intermediate progenitor cells or neurons at 16–18 weeks gestation. Transcriptomic profiling indicates that *SLC12A2* expressing cells (at 16–18 weeks gestation) manifest a transcriptomic programme reflecting active neurogenesis. Reduced function of *SLC12A2* may result in an NDD by altering the delicate process of corticogenesis, and/or by dysregulating the excitatory-inhibitory GABA switch.

The phenotype of humans with *SLC12A2* variants has similarities to animal models. An slc12a2 null zebrafish displays collapse of the otic vesicle with reduced endolymph (Abbas and Whitfield, 2009). This paper did not describe

the brain phenotype. The otic malformation in the zebrafish model has relevance to the hearing loss in *SLC12A2* variant carriers. Several *Slc12a2* murine models exist. We initially reported an *Slc12a2* null mouse with cochlear malformations, loss of hair cells and hearing impairment (Delpire *et al.*, 1999). The brain phenotype in this mouse has not been studied extensively. Reduced neuronal proliferation has been demonstrated in the lateral ganglionic eminence of the null mouse (Magalhães and Rivera, 2016), and NKCC1 knockdown by short-hairpin RNA reduced neuronal proliferation in the murine subventricular zone (Young *et al.*, 2012). The similarities between animal models and the human phenotype of *SCL12A2*, the role of *SLC12A2* in neuronal development, the results of *in silico* analyses and the effects of the SNVs on NKCC1 biochemical function provide strong support for a causal role of *SLC12A2* variants in NDD and BSNHL.

Web resources

https://gnomad.broadinstitute.org/
https://www.networkanalyst.ca/
http://denovolyzer.org/
https://github.com/jeremymcrae/denovonear
https://mupit.icm.jhu.edu/MuPIT_Interactive
https://cadd.gs.washington.edu/
https://decipher.sanger.ac.uk
http://portal.brain-map.org/
https://morlscrnaseq.org/

Funding

Competing interests

The authors report no competing interests.

Supplementary material

Supplementary material is available at *Brain* online.

References

Abbas L, Whitfield TT. Nkcc1 (Slc12a2) is required for the regulation of endolymph volume in the otic vesicle and swim bladder volume in the zebrafish larva. Development 2009; 136: 2837–48.

Arroyo JP, Kahle KT, Gamba G. The SLC12 family of electroneutral cation-coupled chloride cotransporters. Mol Aspects Med 2013; 34: 288–98.

Ben-Ari Y. The yin and yen of GABA in brain development and operation in health and disease. Front Cell Neurosci 2012; 6: 45.

Chen TA, Orlando BJ, Zhang J, Latorraca NR, Wang A, Hollingsworth SA, et al. Structure and mechanism of the cation-chloride cotransporter NKCC1. Nature 2019; 572: 488–92.

Delpire E, Gagnon KB, Ledford JJ, Wallace JM. Housing and husbandry of Xenopus laevis affect the quality of oocytes for heterologous expression studies. J Am Assoc Lab Anim Sci 2011; 50: 46–53.

Delpire E, Lu J, England R, Dull C, Thorne T. Deafness and imbalance associated with inactivation of the secretory Na- K-2Cl co-transporter. Nat Genet 1999; 22: 192–5.

Delpire E, Wolfe L, Flores B, Koumangoye R, Schornak CC, Omer S, et al. A patient with multisystem dysfunction carries a truncation mutation in human SLC12A2, the gene encoding the Na-K-2Cl cotransporter, NKCC1. Cold Spring Harb Mol Case Stud 2016; 2: a001289.

Dixon MJ, Gazzard J, Chaudhry SS, Sampson N, Schulte BA, Steel KP. Mutation of the Na-K-Cl co-transporter gene Slc12a2 results in deafness in mice. Hum Mol Genet 1999; 8: 1579–84.

Green T, Flash S, Reiss AL. Sex differences in psychiatric disorders: what we can learn from sex chromosome aneuploidies. Neuropsychopharmacology 2019; 44: 9–21.

He Q, Nomura T, Xu J, Contractor A. The developmental switch in GABA polarity is delayed in fragile X mice. J Neurosci 2014; 34: 446–50.

Macnamara EF, Koehler AE, D'Souza P, Estwick T, Lee P, Vezina G, et al. Kilquist syndrome: a novel syndromic hearing loss disorder caused by homozygous deletion of SLC12A2. Hum Mutat 2019; 40: 532–8.

Magalhães AC, Rivera C. NKCC1-deficiency results in abnormal proliferation of neural progenitor cells of the lateral ganglionic eminence. Front Cell Neurosci 2016; 10: 200.

McRae JF, Clayton S, Fitzgerald TW, Kaplanis J, Prigmore E, Rajan D, et al. Prevalence and architecture of de novo mutations in developmental disorders. Nature 2017; 542: 433–8.

Miller JA, Ding S-L, Sunkin SM, Smith KA, Ng L, Szafer A, et al. Transcriptional landscape of the prenatal human brain. Nature 2014; 508: 199–206.

Morita Y, Callicott JH, Testa LR, Mighdoll MI, Dickinson D, Chen Q, et al. Characteristics of the cation cotransporter NKCC1 in human brain: alternate transcripts, expression in development, and potential relationships to brain function and Schizophrenia. J Neurosci 2014; 34: 4929–40.

Niknafs N, Kim D, Kim R, Diekhans M, Ryan M, Stenson PD, et al. MuPIT interactive: webserver for mapping variant positions to annotated, interactive 3D structures. Hum Genet 2013; 132: 1235–43.

Plotkin MD, Snyder EY, Hebert SC, Delpire E. Expression of the Na-K-2Cl cotransporter is developmentally regulated in postnatal rat brains: a possible mechanism underlying GABA's excitatory role in immature brain. J Neurobiol 1997; 33: 781–95.

Pollen AA, Nowakowski TJ, Chen J, Retallack H, Sandoval-Espinosa C, Nicholas CR, et al. Molecular identity of human outer radial glia during cortical development. Cell 2015; 163: 55–67.

Ranum PT, Goodwin AT, Yoshimura H, Kolbe DL, Walls WD, Koh JY, et al. Insights into the biology of hearing and deafness revealed by single-cell RNA sequencing. Cell Rep 2019; 26: 3160–71.e3.

Samocha KE, Kosmicki JA, Karczewski KJ, O'Donnell-Luria AH, Pierce-Hoffman E, MacArthur DG, et al. Regional missense

constraint improves variant deleteriousness prediction. bioRxiv 2017: 148353. doi.org/10.1101/148353.

Schwarz JM, Rödelsperger C, Schuelke M, Seelow D. MutationTaster evaluates disease-causing potential of sequence alterations. Nat Methods 2010; 7: 575–6.

Shihab HA, Gough J, Cooper DN, Stenson PD, Barker GLA, Edwards KJ, et al. Predicting the functional, molecular, and phenotypic consequences of amino acid substitutions using hidden Markov models. Hum Mutat 2013; 34: 57–65.

Sobreira N, Schiettecatte F, Valle D, Hamosh A. GeneMatcher: a matching tool for connecting investigators with an interest in the same gene. Hum Mutat 2015; 36: 928–30.

Stranger BE, Brigham LE, Hasz R, Hunter M, Johns C, Johnson M, et al. Enhancing GTEx by bridging the gaps between genotype, gene expression, and disease. Nat Genet 2017; 49: 1664–70.

Urbán N, Guillemot F. Neurogenesis in the embryonic and adult brain: same regulators, different roles. Front Cell Neurosci 2014; 8: 396.

Ware JS, Samocha KE, Homsy J, Daly MJ. Interpreting de novo Variation in Human Disease Using denovolyzeR. Curr Protoc Hum Genet 2015; 87: 7.25.1–.25.15.

Wright CF, Fitzgerald TW, Jones WD, Clayton S, McRae JF, Van Kogelenberg M, et al. Genetic diagnosis of developmental disorders in the DDD study: a scalable analysis of genome-wide research data. Lancet 2015; 385: 1305–14.

Xia J, Gill EE, Hancock R. Networkanalyst for statistical, visual and network-based meta-analysis of gene expression data. Nat Protoc 2015; 10: 823–44.

Young SZ, Morgan Taylor M, Wu S, Ikeda-Matsuo Y, Kubera C, Bordey A. NKCC1 knockdown decreases neuron production through GABAA-regulated neural progenitor proliferation and delays dendrite development. J Neurosci 2012; 32: 13630–8.

Zawerton A, Yao B, Yeager JP, Pippucci T, Haseeb A, Smith JD, et al. De Novo SOX4 variants cause a neurodevelopmental disease associated with mild dysmorphism. Am J Hum Genet 2019; 104: 246–59.